

# A comprehensive AVO classification

ROGER A. YOUNG and ROBERT D. LoPICCOLO, eSeis, Inc., Houston, Texas, U.S.

In this paper a new classification for AVO responses is proposed. This classification covers all possible AVO responses and is independent of the fluid content of the beds.

In 1989 Rutherford and Williams introduced a three-fold classification of AVO (amplitude versus offset) characteristics for seismic reflections from the interface between shales and underlying gas sands. The classification scheme they proposed has become the industry standard and has proven its validity and usefulness in countless exploration efforts.

The Rutherford and Williams classification is primarily based on the sign and magnitude of the reflection coefficient ( $R_0$ ) at the top of the sand. These authors went on to observe that, owing to the high Poisson's ratio values for the typical encasing shales, relative to the gas sands, the AVO response of all of these gas-sand classes would be characterized by an increasingly negative reflection coefficient with increasing offset. Their classification is explicitly defined for gas sands.

In 1997 Castagna and Swan proposed AVO crossplotting wherein an estimate of the normal-incidence reflectivity is plotted against a measure of the offset-dependent reflectivity. Using this approach Castagna and Swan graphically illustrated the continuum between the classes and defined the characteristics of the classes using what they termed AVO intercept and AVO gradient. They also added a class 4, which they believed was originally included in Rutherford and Williams' class 3 definition.

The authors of the present paper propose to expand and partly redefine the currently used classifications. In order to distinguish among the schemes the term types, as opposed to classes, is used to name the different categories. And, in order to preserve congruity, where the schemes overlap, the sands, which Rutherford and Williams would call class 1, 2, or 3, are referred to as types 1, 2, or 3. Type 4 of the proposed classification includes parts of the domains, which Castagna and Swan assigned to their class 4 and their class 3. The proposed classification is intended to provide an unambiguous way of sorting the entire range of combinations of normal-incidence reflectivity and offset-dependent reflectivity, irrespective of the cause of the offset-dependent amplitude variations. A type 5 replaces part of Castagna and Swan's class 4, and types -1 through -5 are added which complete the spectrum.

It is further suggested that AVO effects are best described as being not just between shales and underlying sands, but between nonshale lithologies and the overlying rock (whether it be shale or not). Because nonshale lithology is rather an awkward term, the name "sand" will be used in the following discussion, but the reader is asked to bear in mind that a larger and not especially accurate definition of sand is implied. Clearly, the classification goes beyond gas sands in its intended application. Variation in AVO should be considered a physical phenomenon, the root cause of which requires interpretation.

**AVO types classification.** The new classification is predicated on an analysis of the gradient of the change in amplitude with increasing offset and the value of the intercept of that gradient with the zero-offset or normal-incidence trace. Implicit in the new classification is a tightening of the usage of the term AVO to a more literal definition: analysis of variations in amplitude versus offset.

By making the amplitude variation with offset part of the

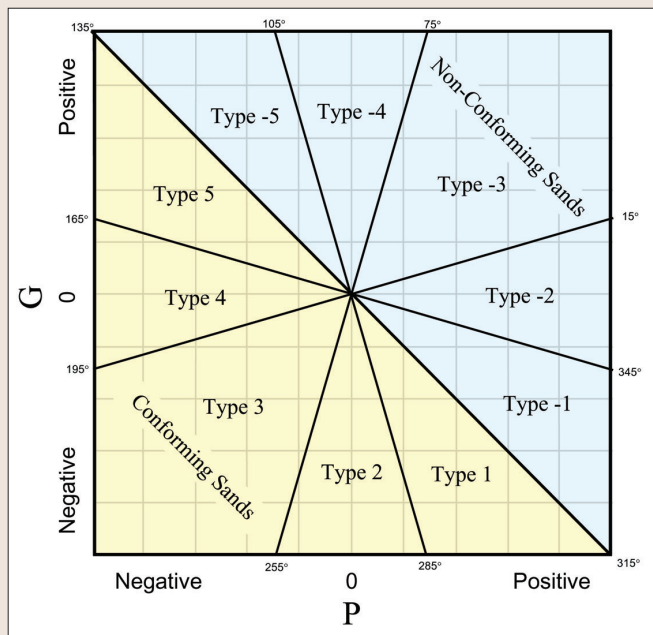


Figure 1. Proposed classification of AVO types as a function of P and G. P and G are both dimensionless and are scaled to have the same range of values.

definition of AVO types, a broader spectrum of combinations presents itself. Reflections may be either positive, negative, or zero and may either increase, decrease, or remain the same with increasing offset.

The present authors endorse Castagna and Swan's AVO crossplotting approach and reproduce their plot, with minor modification, to illustrate the proposed classification (see Figure 1). The ordinate is designated G, defined by fitting a linear approximation to the slope of the amplitude variation with offset and the abscissa is P, defined as the value of the linear approximation at the intercept, where the offset is zero.

In the illustrated construction P and G are both dimensionless and scaled to the same dynamic range. This implies, of course, that how the individual data points fall in the construction of the crossplots may be partly a function of the size and location of the sample taken from the seismic data; there is the possibility that the AVO type assigned to a given reflection may change as a function of the size and location of the sample within which it is included. This is a shortcoming inherent in any AVO classification using this crossplotting approach; it is not unique to the current proposal.

The proposed division boundaries radiate from the origin with a fixed angular relationship (see Figure 1). This basis for divisions has the benefit of being very straightforward to calculate; it also preserves relationships as the sands thin.

The obvious, initial divisions correspond to the four quadrants of the unit circle: P and G are individually either positive or negative and the domains are unique as a function of the combination of these attributes. Four more domains present themselves at and near the boundaries between the quadrants where either P or G will vary little or not at all.

A further division results from the following consideration. If one assumes that the ratio of the P-wave velocity to S-wave velocity in nonhydrocarbon-bearing zones is constant at (approximately) 2 and that the density contrast across reflect-

**Table 1.** AVO types characteristics

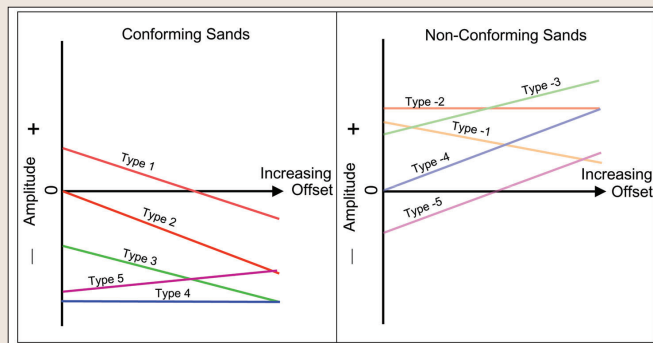
	AVO Type	P (intercept)	G (gradient)	Amplitude vs. Offset
Conforming Sands	1	Positive	Negative	Peak decreasing in amplitude with offset; becomes a trough in the fars
	2	Near zero	Negative	Nearly transparent becoming trough; amplitude increases with offset
	3	Negative	Negative	Trough increasing in amplitude with offset
	4	Negative	Flat	Trough changing little in amplitude with offset
	5	Negative	Positive	Trough decreasing in amplitude with offset
Nonconforming Sands	-1	Positive	Negative	Peak decreasing in amplitude with offset
	-2	Positive	Flat	Peak changing little in amplitude with offset
	-3	Positive	Positive	Peak increasing in amplitude with offset
	-4	Near zero	Positive	Nearly transparent becoming peak; amplitude increases with offset
	-5	Negative	Positive	Trough decreasing in amplitude with offset; becomes a peak in the fars

ing horizons is negligible (as discussed by Foster, Keys, and Reilly, 1997) then the division between positive (1 through 5) and negative (-1 through -5) AVO types corresponds to the linear fluid line of Foster (et al., 1997). As illustrated in Figure 1 sands which fall to the southwest of that line (positive AVO types in the present paper) are described as “conforming sands” in that the effects of decreasing salinity and increasing gas content are similar: Sands are displaced to the southwest by either of these phenomena. In “nonconforming sands” there may be no discernible gas effect, if there is a gas effect it is unchanged from the conforming sands, it tends to displace points to the southwest; the shale effect is the opposite, and decreasing salinity tends to displace points to the northeast.

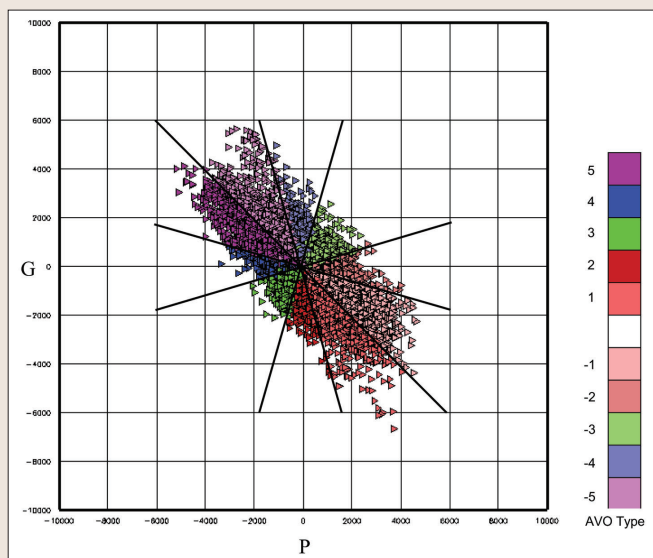
The primary division between types 1 through 5 and the symmetrically opposite types -1 through -5 is at a positive 45° angle to the ordinate (a line trending from 135 to 315° on the unit circle). Type 1 is defined as points lying between 285 and 315° and a type -1 corresponds to 315 through 345°; these two types fill most of the fourth quadrant and are somewhat similar in their responses, with type 1 expressing more variation in (negative) G and type -1 more variation in P. Type 2 AVOs span the next 30° from 255 to 285° where values of P are small, and G is negative. Type 3 occupies most of the third quadrant from 195 to 255° where values of P and G are both negative. Type 4 spans the range 165-195°, where values of P are negative, and G is small. The types 5 and -5 fill most of the second quadrant and correspond to 135-165° and 105-135°, respectively; these types are also similar in their response, with type 5 being more dominated by variations in (negative) P and type -5 being more dominated by variation in G. Type -4 falls on the boundary between the first and second quadrants, at 75-105° and is characterized by small values of P and positive values of G. Type -3 dominates the first quadrant from 15 to 75°, where both P and G are positive. Type -2 ranges from 15 to 345° and is characterized by small changes in G and positive values for P.

Table 1 describes the 10 AVO types included in the proposed classification. The AVO types are also illustrated graphically in Figure 2, which shows the general relationships between the amplitude and offset for all of the types.

In order to calculate AVO types for classification using the proposed scheme we apply the following procedure. An appropriately trimmed, muted, moved-out, and migrated set of gathers is analyzed on a sample-by-sample basis. A least-squares, best-fit line is fitted to the amplitudes. The slope of the line gives G and the intercept of the line, when projected back to the ordinate, gives P. The values of P and G are used to calculate a position on the unit circle and the AVO type is found in a look-up table. An example of the results of this type of calculation is illustrated in Figure 3 by crossplotting color-



**Figure 2.** General relationships between the amplitude of the reflection at normal incidence and the amplitude of the reflections with increasing offset for the different AVO types.



**Figure 3.** Scatter plot showing distribution of real data set evaluated using the proposed classification scheme. Each sample in the seismic data set is evaluated for P and G; the whole set of Ps and Gs is scaled; and the points are plotted accordingly. Color codes are assigned according to the divisions laid out in Figure 1 (and reproduced by the diagonal black lines here). The color-coded points may then be output using an appropriate SEG Y format and displayed as record sections.

coded values of P and G. Finally, a lithology template is created and the shale (or shaley lithologies) are masked out. Thus, in effect, AVO type becomes an instantaneous attribute of the seismic data. The association with nonshale lithologies is important and is kept in the classification because these rocks provide most of the reservoirs of interest.

The salient differences between this scheme and the ear-

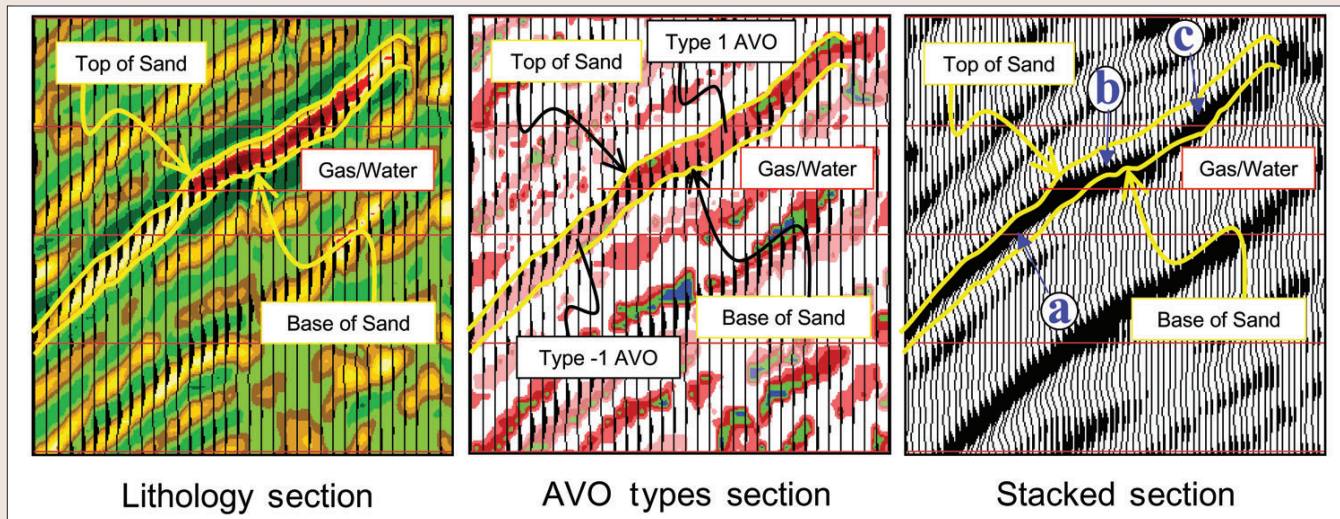
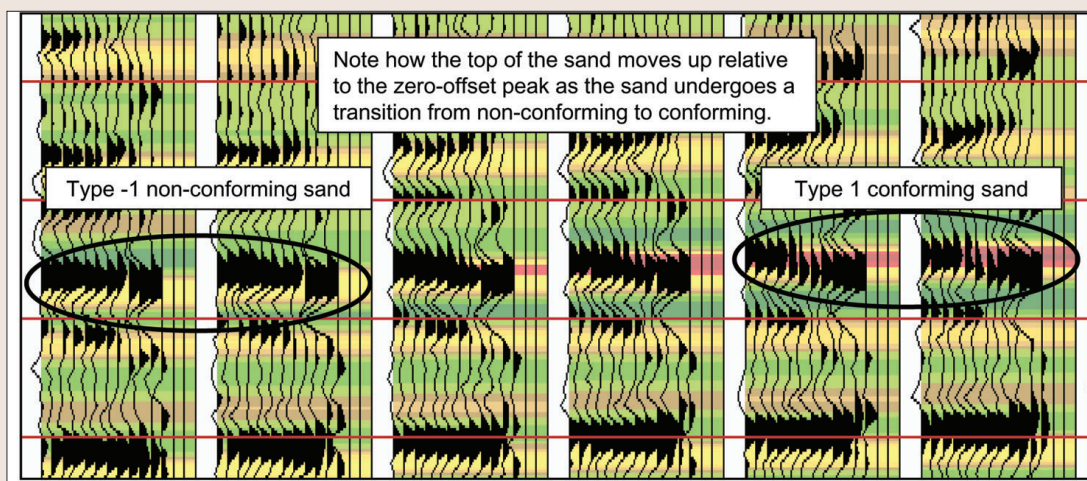


**Figure 4.** Overpressured gas sand with gas water contact. A sand bed (outlined in yellow) displays nonconforming, type -1 AVO characteristics in a down-dip position; the presence of gas in the updip portions of the bed causes it to become conforming and display type 1, 2, and 3 AVO characteristics. The letters a, b, and c on the stacked section refer to the arm, palm, and fingers of the "cupped hand" as described in the text. Every second trace from the stack is superposed on the AVO types and lithology sections. Data courtesy of Fairfield Industries Inc.

**Figure 5.** Panels of gathers showing change in AVO types for an overpressured sand with a gas water contact. A type -1 is illustrated in the two panels on the left side. A type 1 is well-defined in the two panels on the right side. Gathers are taken from the example illustrated in Figure 4 and the lithology in the background is also from Figure 4. Data courtesy of Fairfield Industries Inc.



lier ones are as follows:

- Sands (nonshale lithologies) are designated to be conforming or nonconforming.
- The field of conforming sands is redivided to include a fifth type.
- The AVO types are defined using an angular division of a unit circle inscribed in the field of Ps and Gs.
- AVO type is a continuously distributed property of the seismic data.

**Examples of usage.** The proposed classification permits the easy calculation of the AVO types, which can then be presented in SEGY format. By combining this information with knowledge of the geology of the area, attractive exploration targets can be more easily and accurately identified.

Modeling studies suggest that all 10 AVO types of sands (nonshale lithologies) should exist. More of the implications of the various types will be explored in future publications. However, a few examples are included here to illustrate the application and efficacy of the proposed approach.

Three examples from different parts of the world are presented in Figures 4 through 10. Each example includes sections showing lithology, AVO types, and gathers. Stacked sections are included in two of the examples, and traces extracted from the stack are superposed on all of the lithol-

ogy and AVO types sections. Lithology sections are formulated using a proprietary technology based on AVO analyses, inversions, and crossplotting; however, any suitably accurate technique for establishing the geometry of nonshale lithologic units would suffice. Color-coding for the lithology sections is the same for all of the illustrations: shales are shades of green; sands range from brown to yellow (as they become less shaly); and compressible fluids (gas) are indicated by red. The AVO types are calculated as described elsewhere in this paper; the color bar for the sections is the same as the color bar presented in Figure 3.

In overpressured sediments, nonconforming wet sands are generally the rule with pay sands usually appearing as conforming sands of AVO type 1 to 3. Figure 4 illustrates an example of a transition from a down-dip, nonconforming AVO type -1 to a conforming sand (comprised of AVO types 1, 2, and 3) where it is gas-filled in the updip position. The down-dip portion of the sand in this example has a high impedance relative to the overlying shale. The impedance contrast decreases with increasing offset but remains positive throughout the entire offset range (see Figure 5, left two panels). This is consistent with the form of a type -1 (see Figure 2) and the resulting stack shows a peak associated with the top of the sand.

In the updip portions of the sand the addition of gas has decreased the impedance contrast. More importantly the addition of gas causes the impedance to decrease much more

**Figure 6.** Gas-bearing sand underlying a tight sand. This composite image shows lithology, gathers, and a well log analysis, with every second wiggle trace from the stacked section; insets on the left show gathers with lithology and AVO types in the background. A third inset shows the time-scaled lithology interpretation from a well drilled, at the location marked, plus a set of synthetic traces; the tie between the stratigraphy, the lithologic interpretation, and the AVO types is demonstrated. Carbonate-rich rocks are colored blue on the well log.

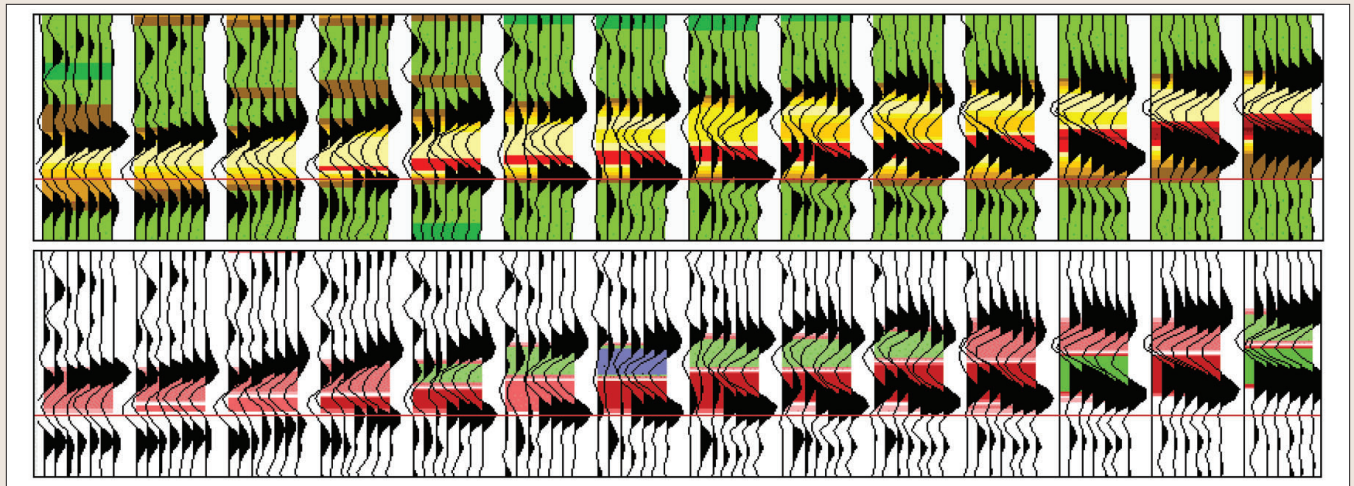
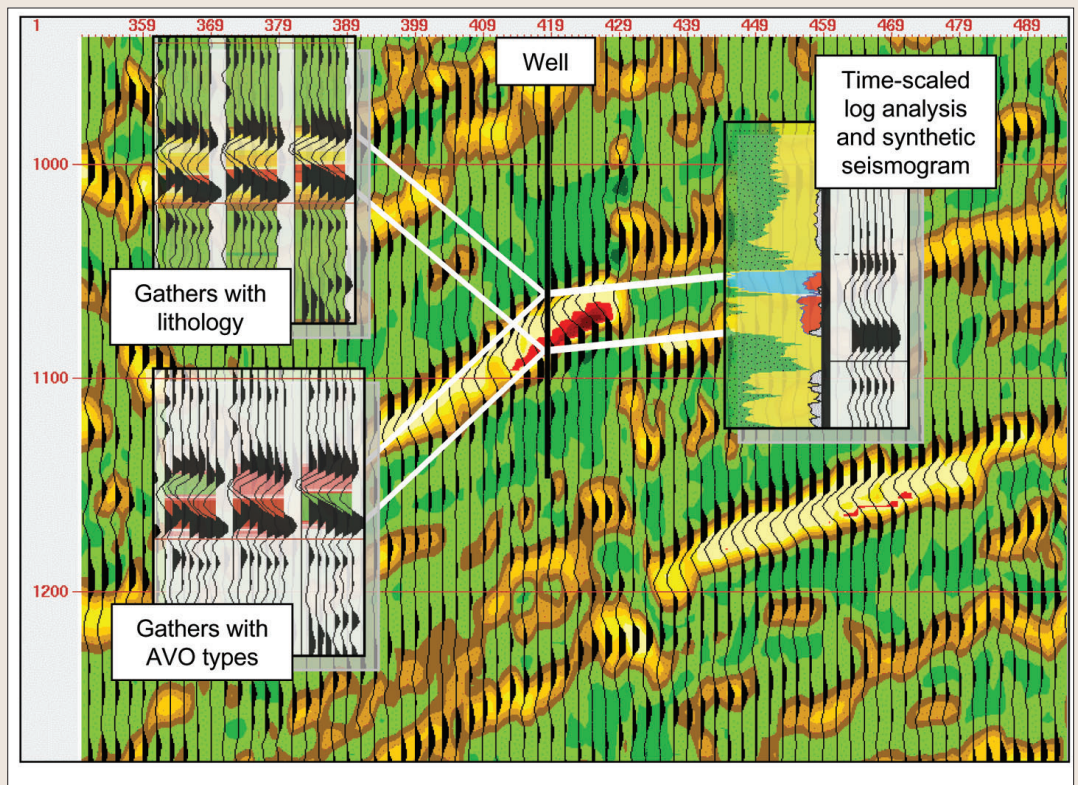


**Figure 7.** Panels of gathers showing change in AVO types with a change in lithology for a gas-bearing sand underlying a tight sand. Gathers are taken from the vicinity of the gas-water contact in the example illustrated in Figure 6. The gathers are superposed on lithology at the top and AVO type at the bottom; lithology and AVO type are from Figure 6. The top of the calcite-cemented, nonconforming sand is characterized by AVO types -2, -3, and -4: all positive amplitudes either increasing with offset or remaining flat. The porous, conforming, lower sand is characterized by AVO types 2, 3, and 4: all negative amplitudes either increasing or remaining flat with offset.

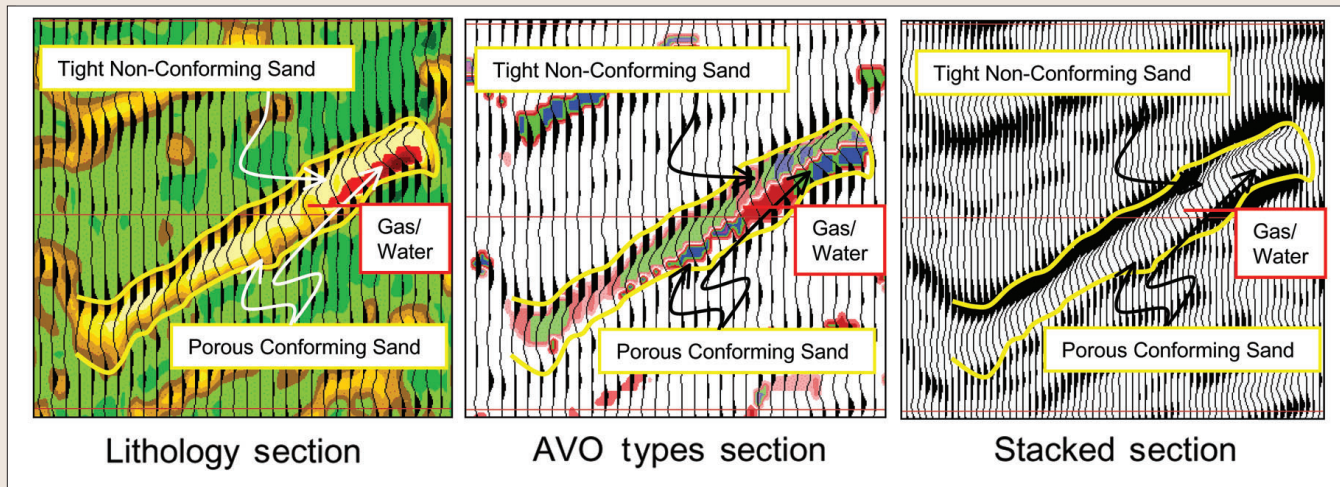
sharply with offset and to become negative in the farther offset ranges (Figure 5, right two panels). This is characteristic of a type 1 AVO (Figure 2) and the stacked reflection associated with the top of the sand weakens; not too far updip of the gas-water contact (see Figure 4), the top of the sand is associated with a trough on the stack, which is characteristic of AVO types 2 and 3.

The transition from a nonconforming to a conforming sand often looks like the cupped palm of a hand facing upward on the stack. In this analogy the arm is the peak at the top of the downdip, wet, nonconforming sand; the palm is formed by the gas-water contact; and the fingers are the peak, which forms the base of the gas-filled portion of the sand. This signature is a powerful, direct hydrocarbon indicator, but it is uncommon and can cause confusion regarding structure or

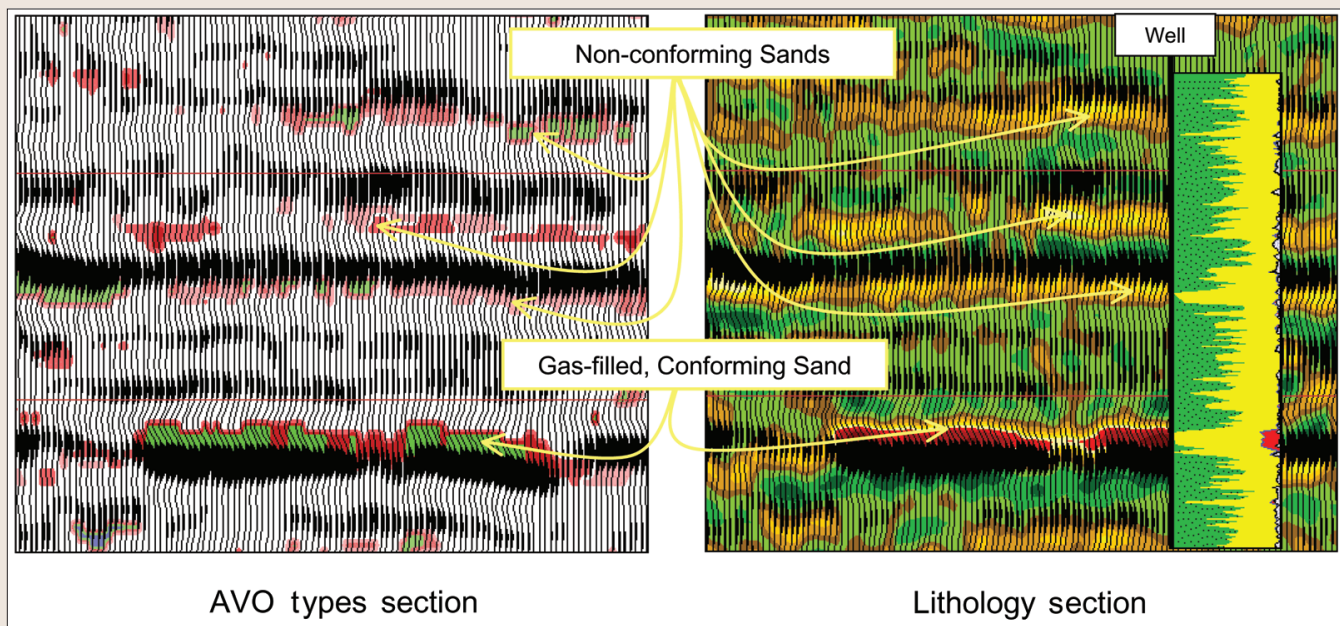
stratigraphy if the root causes are not understood. It is especially interesting to note in Figure 4 that the top of the sand is in a trough where the sand is conforming and in a peak where it is nonconforming. Without an AVO analysis, aided by some rationalizing system, a strong temptation would be to interpret a small fault, offsetting a tight sand (peak over trough).

Figure 6 presents the second example, in which a 75-foot thick, moderately porous gas sand is overlain by a thin, marly shale and a 55-foot thick, tight, calcite-cemented, coquinoid (in places), sandstone.

The top part of the sequence is characterized by a variety of AVO types and all are of the nonconforming variety. Figure 7 shows the gathers from the sand package, highlighted in Figure 6, in the vicinity of the gas-water contact. The top of



**Figure 8.** Detail on Figure 6 of gas-bearing sand underlying a tight sand. A sand section (outlined in yellow) displays nonconforming, AVO types (indicated by pastel shades in middle panel) in the top portion, where it is heavily cemented with calcite and conforming AVO types (indicated by bright colors in middle panel) in the bottom portion, where it is porous and contains a gas-bearing reservoir lying on water. Every second trace from the stack is superposed on the AVO types section.



**Figure 9.** AVO types and lithology sections illustrating conformable and nonconformable sands in separate beds. The upper beds are relatively well-lithified and tight, while the lower bed is gas-filled and relatively more porous. The nonconformable sands range from AVO types  $-1$  to  $-3$  and show a characteristic peak over trough relationship in the stack, whereas the conformable sand is dominantly AVO type 3 and characterized by a trough over peak relationship in the stack. Color bar for the AVO types section is the same as in Figure 3; shales are green, sands are brown to yellow, and gas sands are red in the lithology section.

the package is dominated by a reflection, which generally shows increasing positive amplitude with increasing offset: a hallmark of type  $-3$  and  $-4$  AVOs (see Figure 2), as shown in the lower set of panels. The stack of these gathers shows the characteristic peak associated with the top of a hard sand (Figure 8).

The bottom part of the sequence is mostly types 3 and 4 in the pay zone and in the downdip, wet interval; the gas-water contact seems to be associated with a type 2 AVO (Figure 8). The type 2 AVO response around the gas-water contact may be the result of some energy being reflected from the contact or from diagenesis associated with the contact.

In this instance the tempting interpretation, from the stack, would be the slight thickening of a tight sand, truncated updip by a large regional fault. A rigorous and systematic AVO analysis reveals the correct relationships.

A third example (Figure 9) shows a series of interbedded

sands and shales from a Cretaceous passive margin sequence. Relatively tight, nonconforming sandstones characterize the upper part of the illustrated sequence. AVO types in the upper sandstone range from  $-1$  to  $-3$  and the tops of the sands are associated with peaks, which show either a slight increase, decrease, or remain fairly constant with offset (Figure 10). By contrast the gas-bearing sand in the lower part of the illustration is dominantly an AVO type 3 with a strong trough-over-peak showing some increase in absolute amplitude with offset. The ability to assign AVO types to the reflected energy and then to interpret the significance of the AVO type with respect to lithology allows the interpreter to be more sophisticated in sorting out tight, porous, and gas-bearing sands.

In all of the foregoing examples the indicated pay zones have been drilled and confirmed; the downdip lithologies in the first two examples are corroborated by the known geology of the area, but not by drilling on the lines.

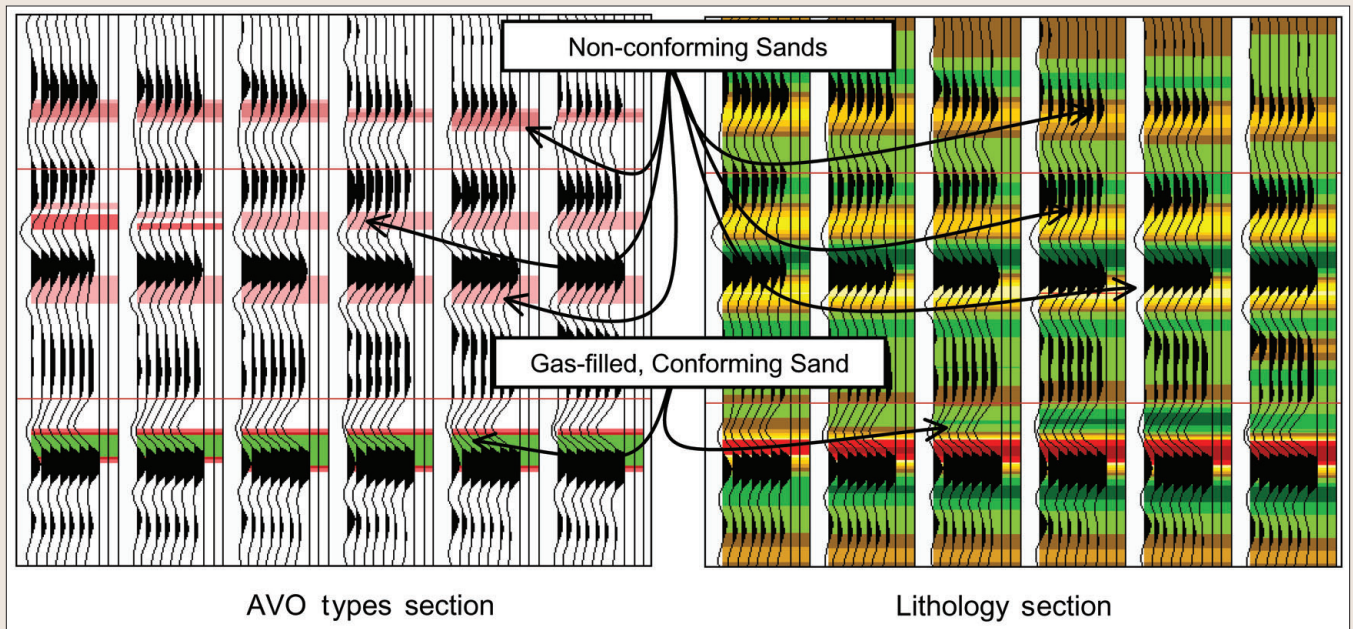


**Figure 10.** Gathers from the vicinity of the well in Figure 9 superposed on AVO types and lithology sections. The upper beds are relatively well-lithified and tight, while the lower bed is gas-filled and relatively more porous. The nonconforming sands are mostly AVO type -1 and -2, characterized by a peak either losing amplitude or remaining flat with offset. The conforming sand is dominantly AVO type 3 characterized by a trough increasing slightly with offset. Color bar for the AVO types section is the same as in Figure 3; shales are green, sands are brown to yellow, and gas sands are red in the lithology section.

**Summary.** An AVO classification is proposed wherein all possible combinations of normal-incidence reflectivity and offset-dependent reflectivity, for all seismic energy coming from the top of nonshale lithologies, are subdivided into 10 types. Broadly, the divisions result from dividing a unit circle into eight domains depending on the attributes of P and G: They each may be positive, near zero, or negative, independently of the other. Two of the domains are further subdivided and all of the domains are grouped by a further distinction as to whether the types are: conforming, where decreasing shaliness and increasing gas have similar effects; or, nonconforming, where decreasing shaliness and increasing gas have opposite effects (or gas has no effect). The definitions are divorced from a gas-sand association and applied, without discrimination, to any nonshale lithology. This approach also departs from conventional AVO analyses in that the AVO attribute becomes a continuously distributed attribute of the seismic data.

Three examples of the application of this classification demonstrate insights into the geology, which otherwise would have been difficult or impossible.

**Suggested reading.** "Principles of AVO crossplotting" by Castagna and Swan (*TLE*, 1997). "Another perspective on AVO crossplotting" by Foster et al. (*TLE*, 1997). "Amplitude-versus-offset variations in gas sands" by Rutherford and Williams (*GEOPHYSICS*, 1989). [TLE](#)

*Acknowledgments:* Authors acknowledge anonymous clients and Fairfield Industries Inc. (Figures 4 and 5) for permission to use examples from their data. We also thank Taylor Lepley, Gordon Van Swearingen, David Reinkemeyer, Linda Young, Tim Schaaf, and Bob Davis for discussions and critical reviews.

Roger A. Young is a cofounder and chief technology officer of eSeis, Inc. He holds an MS in petroleum engineering from the University of Houston.

Robert D. LoPiccolo is president of eSeis, Inc. He holds a PhD in geology from Louisiana State University.

Corresponding authors: [ryoung@e-seis.com](mailto:ryoung@e-seis.com); [lopic@e-seis.com](mailto:lopic@e-seis.com)